

[see commentary on page 259](#)

Loss of heparan sulfate glycosaminoglycan assembly in podocytes does not lead to proteinuria

Shoujun Chen¹, Deborah J. Wassenhove-McCarthy², Yu Yamaguchi³, Lawrence B. Holzman⁴, Toin H. van Kuppevelt⁵, Guido J. Jenniskens⁵, Tessa J. Wijnhoven^{5,6}, Ann C. Woods⁷ and Kevin J. McCarthy^{1,2}

¹Department of Cell Biology and Anatomy, Louisiana State University Health Sciences Center, Shreveport, LA, USA; ²Department of Pathology, Louisiana State University Health Sciences Center, Shreveport, LA, USA; ³Tumor Microenvironment Program, NCI Cancer Center, Burnham Institute for Medical Research, La Jolla, CA, USA; ⁴Department of Medicine, School of Medicine, University of Michigan, Ann Arbor, MI, USA; ⁵Department of Biochemistry, Nijmegen Center for Molecular Life Sciences, Radboud University Nijmegen Medical Center, Nijmegen, The Netherlands; ⁶Department of Pediatric Nephrology, Nijmegen Center for Molecular Life Sciences, Radboud University Nijmegen Medical Center, Nijmegen, The Netherlands and ⁷Department of Cell Biology, School of Medicine, University of Alabama at Birmingham, Birmingham, AL, USA

Podocytes synthesize the majority of the glomerular basement membrane components with some contribution from the glomerular capillary endothelial cells. The anionic charge of heparan sulfate proteoglycans is conferred by covalently attached heparan sulfate glycosaminoglycans and these are thought to provide critical charge selectivity to the glomerular basement membrane for ultrafiltration. One key component in heparan sulfate glycosaminoglycan assembly is the *Ext1* gene product encoding a subunit of heparan sulfate co-polymerase. Here we knocked out *Ext1* gene expression in podocytes halting polymerization of heparin sulfate glycosaminoglycans on the proteoglycan core proteins secreted by podocytes. Glomerular development occurred normally in these knockout animals but changes in podocyte morphology, such as foot process effacement, were seen as early as 1 month after birth. Immunohistochemical analysis showed a significant decrease in heparan sulfate glycosaminoglycans confirmed by ultrastructural studies using polyethyleneimine staining. Despite podocyte abnormalities and loss of heparan sulfate glycosaminoglycans, severe albuminuria did not develop in the knockout mice. We show that the presence of podocyte-secreted heparan sulfate glycosaminoglycans is not absolutely necessary to limit albuminuria suggesting the existence of other mechanisms that limit albuminuria. Heparan sulfate glycosaminoglycans appear to have functions that control podocyte behavior rather than be primarily an ultrafiltration barrier.

Kidney International (2008) **74**, 289–299; doi:10.1038/ki.2008.159; published online 14 May 2008

KEYWORDS: *Ext1*; heparan; proteoglycan; glycosaminoglycan; podocyte; glomerulus

Correspondence: Kevin J. McCarthy, Department of Pathology, Louisiana State University Health Sciences Center, 1501 Kings Highway, Shreveport, LA 71106, USA. E-mail: kmccar2@lsuhsc.edu

Received 17 April 2007; revised 7 February 2008; accepted 12 February 2008; published online 14 May 2008

Proteoglycans (PGs) can be considered to be hypervariable molecules with respect to structure and function; the hypervariability being conferred by information contained in the nature of the core protein and in the covalently attached glycosaminoglycan (GAG) chains.¹ Changes in the pericellular microenvironment affect not only the levels of synthesis of PG core proteins but also the organization of critical elements within the GAG chains, such as carbohydrate composition, sulfation, and epimerization.² Research on PGs over the past 25 years has allowed the scientific community to move beyond the past conceptual constraints that relegated PGs to simple structural elements in the extracellular matrix. Most researchers now embrace the fact that PGs serve many critical functions in tissues, such as control of cell differentiation, migration, and adhesion.³

In the field of renal biology, the classic experiments of Kanwar *et al.*⁴ provided the foundation from which a paradigm evolved that supported the concept that heparan sulfate (HS)-GAG chains on HSPGs served as a filtration medium in the glomerular capillary wall. Using short-term heparanase III treatment to eliminate HS-GAG chains from the glomerular capillary basement membrane (GBM), they were able to alter the permselectivity of the GBM to native ferritin. The results led Kanwar *et al.* to postulate that the highly negative charged HS-GAGs served to impart charge selectivity to the filtration barrier in the kidney. Since that first report, numerous other studies using similar and alternative approaches had, in part, validated this observation. Subsequent studies made an association between the loss of HS-GAGs from the glomerular capillary wall and the development of albuminuria in the progression of nephropathy in individuals afflicted with long-term, poorly controlled diabetes.

The assembly of HS-GAG on PG core proteins is a processive biosynthetic event involving at least five separate glycosyltransferases, sulfotransferases, and epimerases (Figure 1).

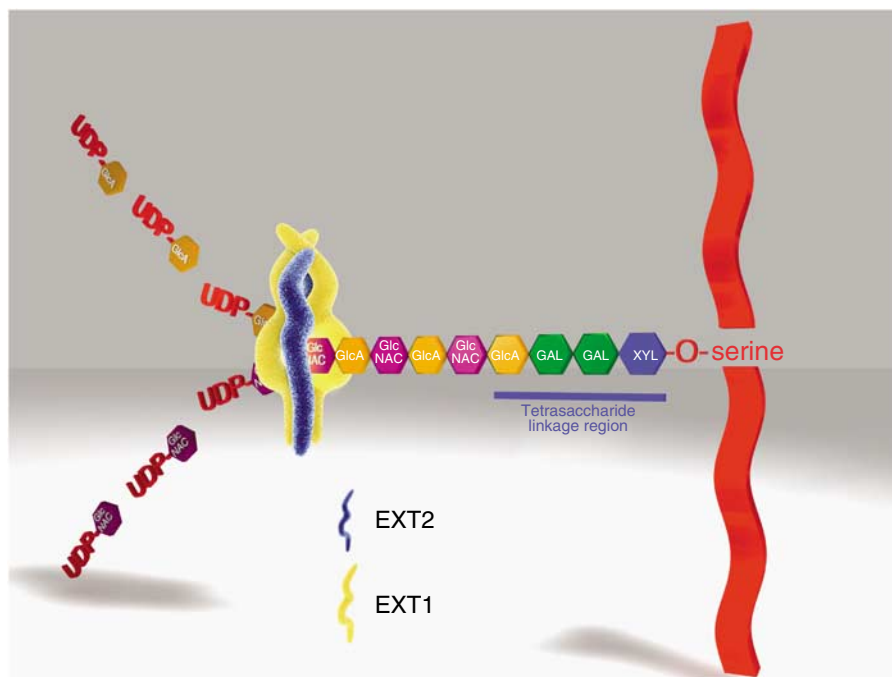


Figure 1 | The cartoon depicts a simplified scheme of the assembly and extension of HS-GAG chains on a PG core protein. The initial step in the assembly of the HS-GAG chain (and common to all HS and chondroitin sulfate-bearing PGs) is the assembly of a linker tetrasaccharide (glucuronosyl- β 1,3-galactosyl- β 1,3-galactosyl- β 1,4 xylose) attached to a serine residue present in the proteoglycan core protein. Each carbohydrate residue in the linkage region is assembled by a specific glycosyltransferase. In the case of HS-GAG, following the assembly of the linkage region, an *N*-acetyl glucosamine residue (α -GlcNAc) is the next carbohydrate residue attached to the linkage region by the enzyme EXTL3. Once assembled, the pentasaccharide is recognized by heparan sulfate copolymerase, EXT1/EXT2. The HS copolymerase extends the nascent GAG chain by the sequential addition of a glucuronic acid (UA) and *N*-acetyl glucosamine (GLN), which are derived from UDP precursors, forming a repetitive copolymer of these subunits (GlcNAc α 1-4GlcA β 1-4) $_n$. For the sake of simplification, the subsequent events in the process, such as deacetylation, sulfation, and uronic acid epimerization, which occur during HS chain elongation are not depicted.

Initially a common linkage region of glucuronic acid-galactose-galactose-xylose (GlcA β →1,3 Gal β →1,3 Gal β →1,4 Xyl β -) is assembled on a core protein serine residue. Once this four carbohydrate linkage region is assembled, an additional GlcNAc is added by the EXTL3 enzyme.⁵ Subsequent heparan chain elongation/polymerization occurs by the actions of the HS-copolymerase EXT1/EXT2.⁶ Of the two enzymes present in the copolymerase, the absence of EXT1 from the copolymerase results in complete loss of the HS polymerase activity.

The major biosynthetic source of basement membrane (BM) material in the glomerular capillary wall has been thought to be the visceral epithelial cell, or podocyte, which resides on the external surface of the glomerular capillary wall.^{7,8} Using a Cre-lox approach, we mutated the *Ext1* gene in glomerular podocytes by selectively breeding mice in which loxP sites flanked exon 1 of the *Ext1* allele (*Ext1*^{flxed/flxed})⁹ with mice transgenic for Cre recombinase, the expression of which was driven by a podocin (NPHS2) promoter (2.5P-Cre mice¹⁰). Since podocin is only expressed in podocytes within the renal glomerulus, the 2.5P-Cre promoter construct leads to podocyte-specific expression of Cre recombinase. For the sake of brevity, the resultant mutant mice (2.5P-Cre, *Ext1*^{flxed/flxed}) have been called PEXTKO mice (podocyte-specific *Ext1* knockout; Figure 2).

RESULTS

The fact that activation of the podocin gene does not occur in podocytes until the capillary loop phase of nephrogenesis¹⁰ led us to predict that the basic process of nephrogenesis should be unaffected in PEXTKO animals, the consequences of the targeted knockout occurring downstream during subsequent glomerular growth and maturation. Predictably, if the sole function of HS-GAGs attached to PG core proteins within the GBM was to determine size/charge selectivity for glomerular ultrafiltration, the effects of eliminating HS-GAG should have resulted in postnatal lethality (3–4 weeks) from severe proteinuria in a manner similar to that had been shown in a laminin β 2 knockout animal model.¹¹ Surprisingly, no perinatal morbidity and lethality were seen in any of the PEXTKO animals. Body weights and combined kidney weights did not show a statistically significant difference in young (2 months) or older (8 months) PEXTKO animals when compared to control. Renal hypertrophy, as indicated by the kidney weight/body weight ratio was not seen in young animals (2 months), but was significant in PEXTKO animals at 8 months of age when compared to controls (Figure S1).

Our initial routine light microscopy examination of kidneys taken from 1- and 3-month-old control and PEXTKO animals did not show any differences (Figure 3a–d).

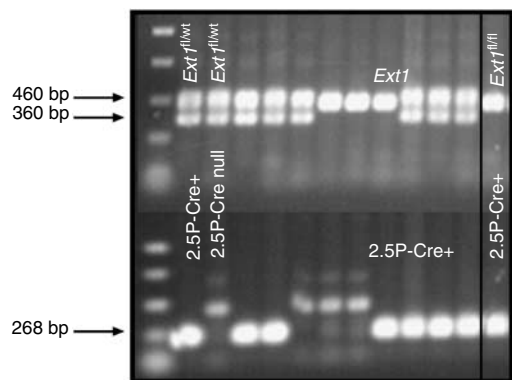


Figure 2 | The results of a PCR-based genotype screen for the presence of *Ext1*^{fl/fl} alleles and the 2.5P-Cre transgene.

Amplification of the wild-type *Ext1* allele (*Ext1*^{wt}) yields a product of 360 bp, whereas the *Ext1*^{fl/fl} allele yields a larger 460-bp product. The 2.5P-Cre product is 268 bp. The boxed-in area of the gel represents an animal with the PEXTKO genotype.

As the animals aged, the proximal tubule epithelial cells developed an abnormal vacuolated cytoplasm (Figure 3f and h). Staining of tissue sections with Oil Red O and with osmium tetroxide (data not shown) was negative, indicating that the vacuoles were not filled with lipid. The presence of vacuoles in proximal tubule epithelial cells was not seen in age-matched controls (Figure 3e, g).

Immunohistochemistry using a monoclonal antibody directed against an epitope present on HS-GAGs (antibody HS4C3; Figure 4a–f)¹² showed a significant, persistent decrease in staining for HS-GAG in the glomerular capillary wall. Glomerular staining for HS-GAG was not entirely abolished within the renal glomerulus, since mesangial cells and capillary endothelial cells would still possess the ability to assemble HS-GAGs. Immunohistochemistry using monoclonal antibodies directed against chondroitin-6 (C-6)-sulfated epitopes (Figure 4g and h) investigated the possibility that one potential default pathway to maintain anionic charge density might be the *de novo* initiation of synthesis/substitution of C-6-sulfated GAGs on PG core proteins. However, there was no apparent difference in the pattern of distribution of C-6-sulfated GAGs between control and PEXTKO animals. By early adulthood (3 months of age; Figure 4i), the glomeruli of PEXTKO animals showed that persistent, significant hypertrophy existed when compared to control animals.

To investigate potential changes in the protein composition of the GBM, tissue sections from 1-, 3-, and 8-month-old animals were immunostained with antibodies against the $\gamma 1$ chain of laminin (not shown), agrin, and perlecan PG core proteins (Figure 5a–l). Despite the hypertrophy seen in PEXTKO glomeruli, there was no readily apparent difference in the intensity nor patterns of immunostaining for $\gamma 1$ laminin (not shown) or perlecan core protein (Figure 5a, b, e, f, i and j). In contrast, glomeruli in the PEXTKO animals had comparatively higher intensities of immunostaining for agrin core protein at every time interval examined (Figure 5c, d, g, h, k and l).

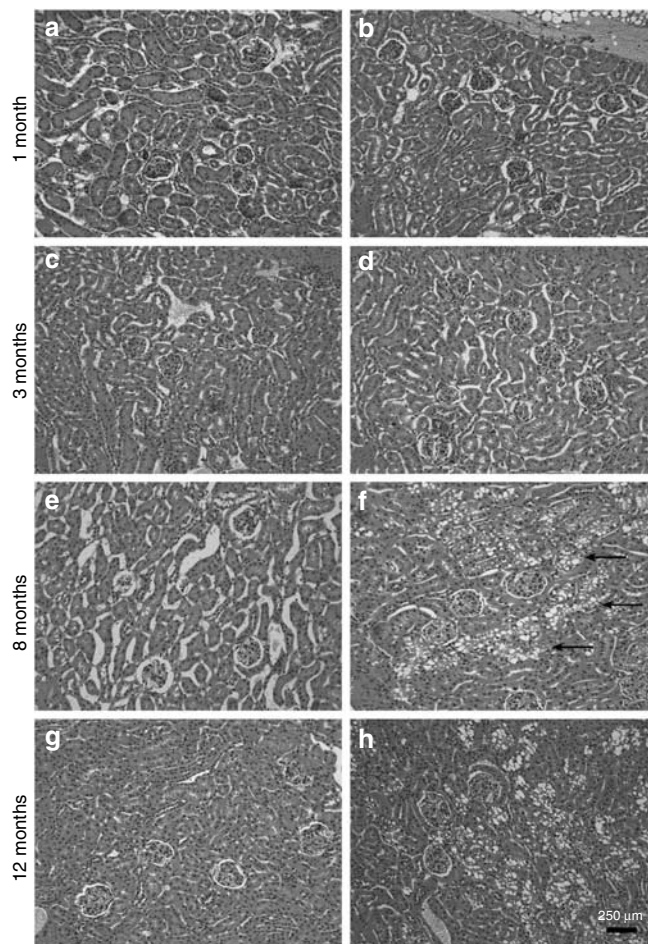


Figure 3 | The micrographs of tissue sections from control (a, c, e, g) or PEXTKO animals (b, d, f, h) stained with hematoxylin and eosin. The age-matched animals were 1 (a, b), 3 (c, d), 8 (e, f), and 12 (g, h) months of age. Overall there were no profound differences in either glomerular or tubular structure between control and PEXTKO kidney at 1 and 3 months of age; no differences among the control animals were seen at any age examined. At 8 months of age, there were very apparent changes in the proximal tubule epithelial cells in the PEXTKO animals (f, arrows), the cells of which had large vacuoles present in the cytoplasm. These changes persisted in older PEXTKO animals (h).

Electron microscopy studies of the glomeruli from PEXTKO animals showed significant ultrastructural changes at 1 month of age (Figure 6b), some of which persisted into adulthood (Figure 7) when compared to age-matched control animals (Figure 6a). In tissue sections from 1-month-old animals, the basic organization of the glomerular podocytes was abnormal, with obvious foot process effacement (Figure 6b) occurring along the perimeter of the GBM. Microvilli were found on the apical surface of the podocytes from 1-month-old animals (Figure 6b). In portions of the glomerular capillary walls in the kidneys of some animals, there were areas where the normal developmental process of glomerular basement ‘fusion’ may have failed to occur, as indicated by the presence of a double BM in the capillary wall (Figure 6b, inset). In addition, the presence of numerous

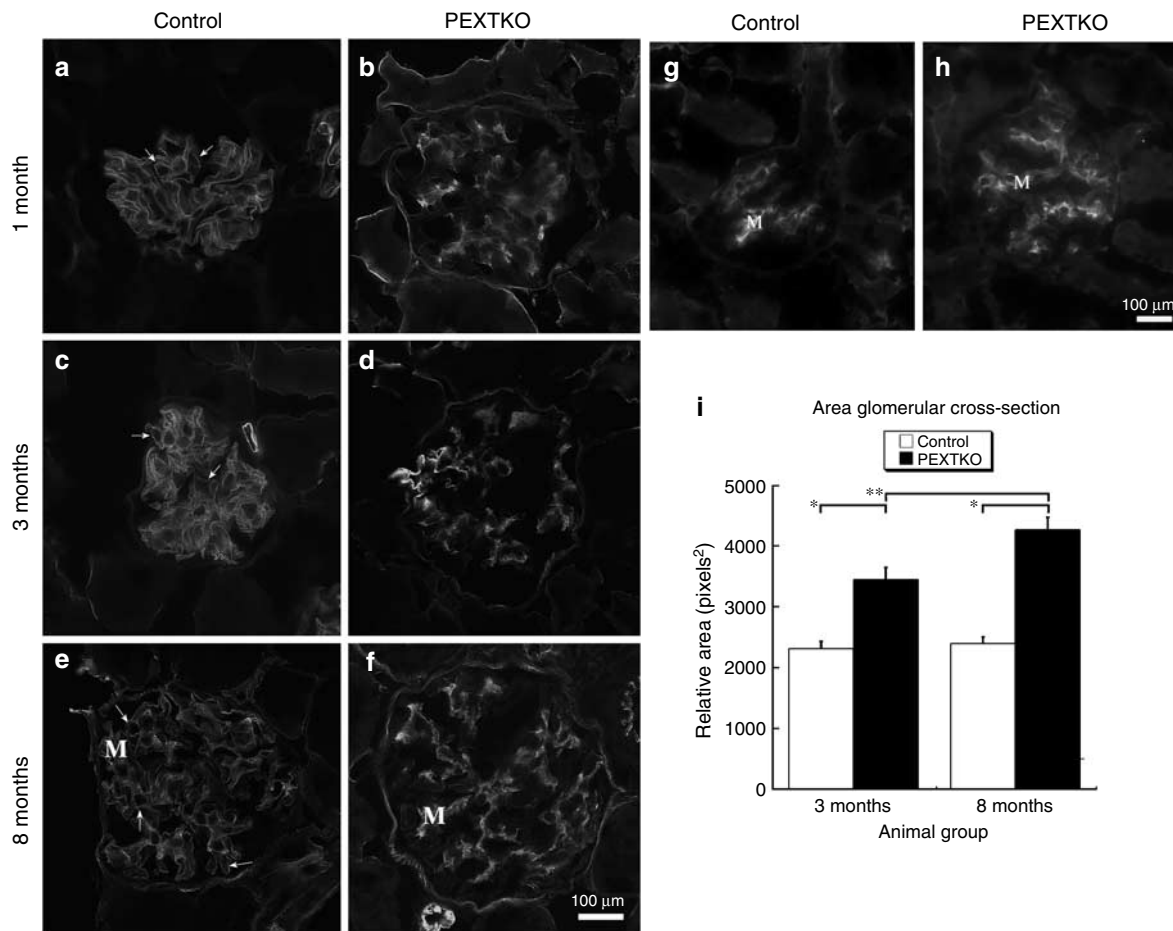


Figure 4 | The micrographs are of tissue sections of kidney immunostained with antibodies against HS-GAGs (antibody HS4C3, a–f) or chondroitin sulfate GAGs (CS-GAGs, antibody 3B3, g, h). (a–f) Deconvolved images resolving a single focal plane, **(b, d, f)** glomeruli from PEXTKO animals of 1, 3, and 8 months of age respectively. **(a, c, e)** Age-matched control animals. **(g, h)** Glomeruli from 3-month-old control and PEXTKO animals, respectively. In control glomeruli **(a, c, e)**, the HS4C3 antibody immunostains the pericapillary (arrows) and perimesangial GBM as well as the mesangial matrix (M). In PEXTKO glomeruli **(b, d, f)**, HS4C3 stains primarily the mesangial matrix (M), with significantly reduced staining in the pericapillary GBM. The glomeruli in **(g)** (control) and **(h)** (PEXTKO) show similar patterns of mesangial staining (M) with no GBM staining, indicating that CS-GAGs were not substituted on GBM proteoglycan core proteins as a default mechanism. **(i)** The results of morphometric measures of glomerular area in control and PEXTKO animals. At both ages examined, the glomeruli from PEXTKO animals were hypertrophic compared to age-matched control animals ($*P < 0.0001$); and glomerular hypertrophy gradually increased over time ($**P < 0.006$).

‘outpockets’ or ‘humps’ of BM material on outside of the glomerular capillary wall was also seen. Although not common in the normal adult glomerulus, during glomerular maturation this particular morphology is indicative of regions of the GBM where newly synthesized material is being spliced into existing GBM.¹³ In older animals (>3 months of age), both ‘outpockets’ of BM material, foot process effacement, and the presence of microvilli persisted (Figure 7) but no evidence of a ‘double’ or ‘split’ BM was seen, suggesting that this particular abnormality may not persist in older animals. Despite changes that would be considered an indicator of glomerular dysfunction, only a minor albuminuria that was not statistically significant relative to controls developed in young (2 months of age) PEXTKO animals (Figure 8). Over time (8 months of age), the albuminuria gradually increased but still was mild and not statistically significant from control animals (Figure 8).

To corroborate the immunohistochemistry data, which showed the loss of HS-GAG from the GBM (Figure 4), polyethylenimine (PEI) staining was done to demonstrate the presence/absence of anionic sites in the GBM (Figure 9a and b). In control animals (Figure 9a and c), PEI labeled the GBM in a consistent ratio of 2:1 lamina rara externa (LRE):lamina rara interna (LRI) sites (Figure 9c). In PEXTKO mice at each age examined, (Figure 9b and c), the number of anionic sites per unit length GBM decreased significantly as did the labeling ratio (1:3 LRE:LRI sites). Thus, the development of a very mild albuminuria in the PEXTKO mouse was gradual, first seen in the 2-month-old animals by ELISA-based assays (Figure 8d) and was associated with foot process effacement and loss of anionic sites in the LRE. Over time, the albuminuria gradually increased but still remained relatively mild, its gradual increase associated with abnormal tubular epithelial

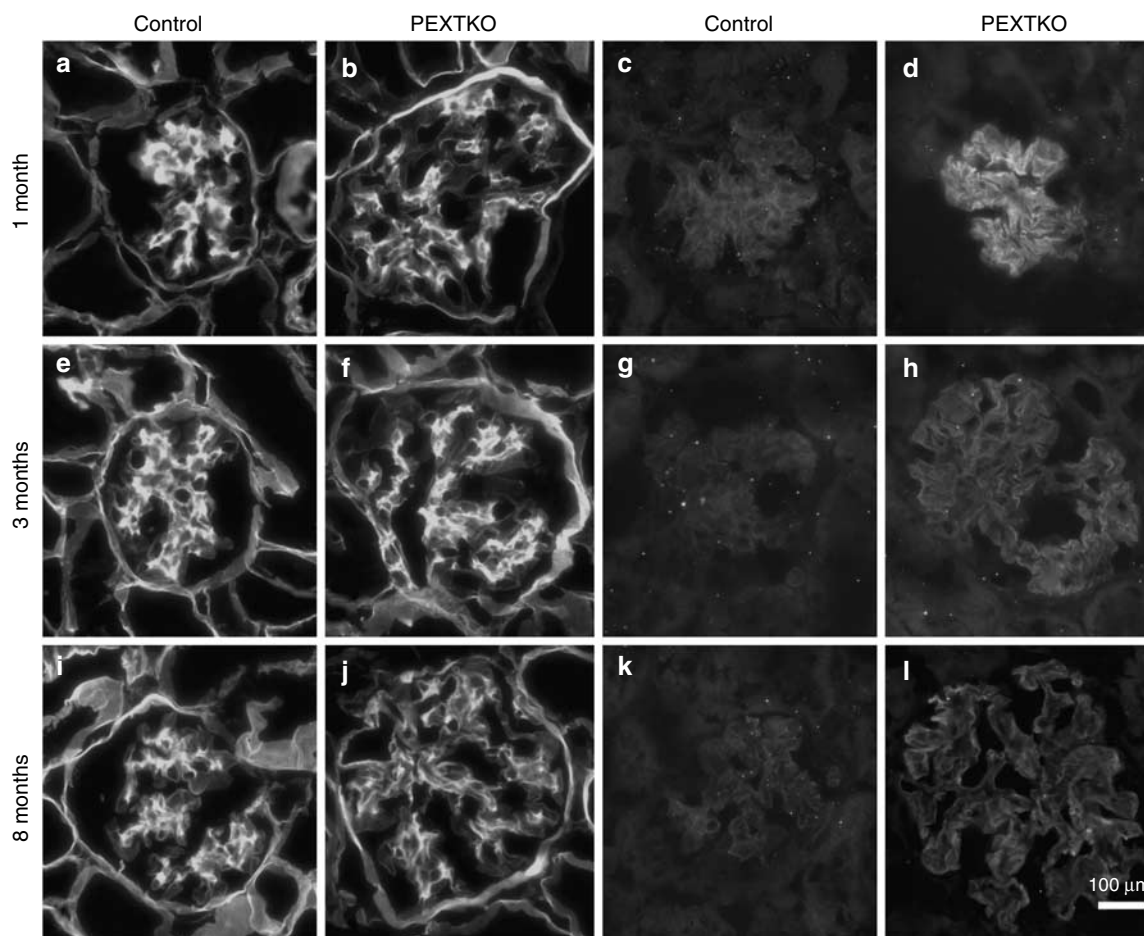


Figure 5 | The micrographs are of tissue sections immunostained with antibodies against either perlecan (antibody A7L6; a, b, e, f, i, j) and agrin (antibody K-17; c, d, g, h, k, l). Glomeruli from control (a, c, e, g, i, k) and PEXTKO animals (b, d, f, h, j, l) are presented in an age-matched manner identical to Figure 1. To show staining intensity differences in the agrin-stained glomeruli, the exposure for each image pair was set to the specimen with the brightest intensity, and both control and PEXTKO images were subsequently imaged at the same exposure setting. For both proteoglycan core protein species, there is no visible change in the pattern of distribution within the glomerulus. The distribution of perlecan staining in both control and PEXTKO animals is identical, being strongest in the mesangial matrix and weaker staining seen in the glomerular capillary wall. In contrast, at each age (1, 3, and 8 months) the intensity for agrin staining in the glomeruli from PEXTKO animals is greater than that seen in the control animals.

morphology (Figure 3f and h), and the persistent loss of anionic sites in the GBM (Figure 9c).

DISCUSSION

At first glance, the renal morphological and functional phenotypes seen in the PEXTKO mouse appears to defy several widely accepted paradigms in the field of renal biology. The data show that despite the selective loss of HS-GAG from the GBM, in particular the LRE, the PEXTKO mice do not appear to develop albuminuria until 2 months of age, the albuminuria being relatively minor. In older animals (8 months), the albuminuria was slightly increased compared to controls but still was relatively minor. To date (>24 months), outside of the experimental protocols, none of the PEXTKO mouse strain animals have suffered any morbidity or mortality.

Several investigations of the glomerular ultrafiltration surface used degradation with specific carbohydrate lyases^{4,14} or neutralization of anionic charge^{15,16} as methods to probe

the function of the carbohydrate elements within the GBM. In contrast to the *in situ* approach of Kanwar *et al.*⁴ which showed that the anionic charge on GBM HS-GAGs conferred charge selectivity to the barrier, a recent study by Wijnhoven *et al.*,¹⁴ which used an *in vivo* approach to remove HS from the GBM, showed that injection of rats with heparanase III did not result in the development of acute proteinuria. Interestingly, *in vivo* digestion of neuraminic acid residues did result in acute proteinuria.

Although these approaches have yielded very significant information about the behavior/function of carbohydrate elements of the GBM, the technical limitations of those studies placed constraints on the temporal interval over which alterations in the dynamic of the nephron and its GBM could be observed. Molecular genetic approaches now permit longer term observation of either global or discrete tissue-specific perturbations of the glycobiology of GBMs. One global approach, which eliminated the primary HS-GAG acceptor

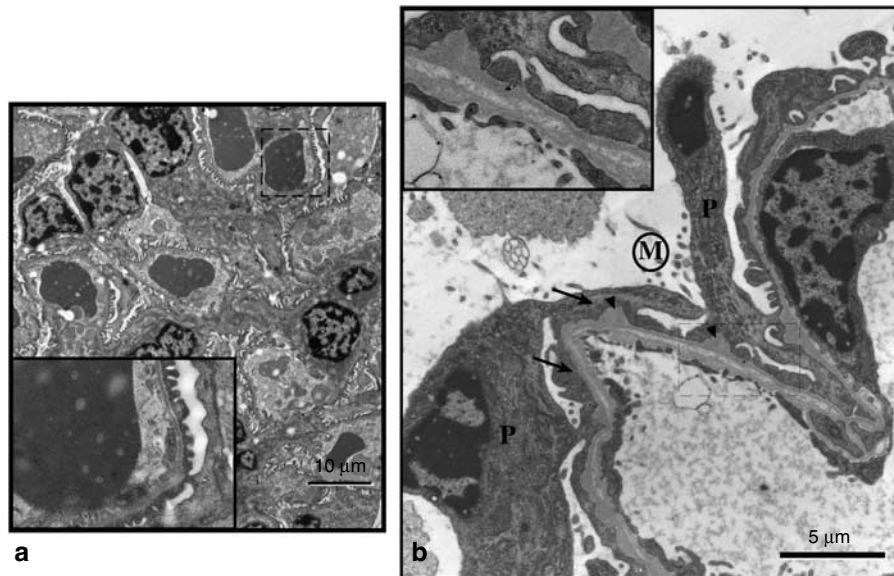


Figure 6 | The electron micrographs show glomeruli from adult control animals (a, 2.5P-Cre + /Ext1^{wt/wt}) and PEXTKO (b, 2.5P-Cre + /Ext1^{fl/fl}) animals. In control animals, the basic architecture of the glomeruli from these animals is normal, with no visible sign of foot process effacement or obvious BM 'outpockets.' The inset in the corner of each larger micrograph is a higher magnification of the area in the main micrograph outlined by the dashed line. (b) An electron micrograph of a glomerular capillary wall from a 1-month-old PEXTKO mouse. Within the picture are the cell bodies of two podocytes (P) having abnormal, effaced foot processes (arrows). On the apical surface of the podocytes, microvilli (area denoted by M) can be found. The GBM also shows irregularities, having numerous outpockets or 'humps' (arrowheads) on the podocyte side of the GBM. The inset shows an enlargement of the boxed-in area of the capillary wall. In this region, the BM has an abnormal appearance, resembling two separate BMs. The presence of the outpockets, along with the double BM, suggests the possibility that GBM fusion, a normal developmental process, has been delayed in this area of the glomerulus. The presence of a double BM has not been seen in older (> 3 months) animals.

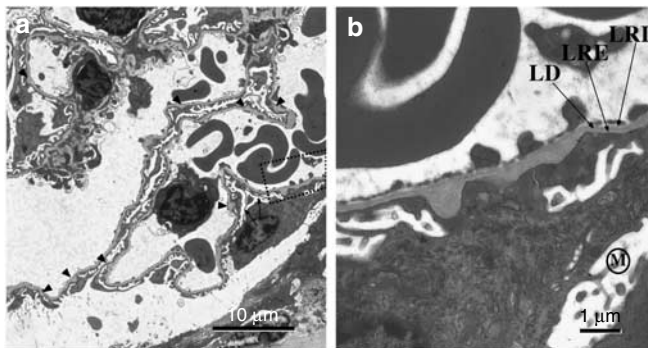


Figure 7 | The electron micrographs map the changes in glomerular capillaries seen in adult (3 months) PEXTKO animals. (a) Low magnification electron micrograph of several glomerular capillaries. The arrowheads in the picture denote areas where there are BM 'outpockets' in the capillary wall. Although in developing/maturing kidneys this type of morphology is associated with areas where active BM synthesis/splicing is occurring, it is also possible that these areas could be areas of basement membrane remodeling by podocytes. The arrows point to two abnormally attenuated primary processes of a podocyte. The boxed-in area of (a) is shown in higher magnification in (b). The apical surface of the podocyte shows the abnormal presence of microvilli (M) and the region of foot process in the basal side of the podocyte is severely effaced. Despite the presence of the 'outpockets' of BM material, in the normal thickness GBM the classic LRE-lamina densa (LD)-LRI organization is easily seen, suggesting that BM assembly may be essentially normal.

site (the HSPG2^{Δ3/Δ3} mouse) within the coding region for the BM PG perlecan,¹⁷ showed minimal effect on glomerular ultrafiltration and podocyte morphology unless a supraphysiologic stressor was placed upon the system.¹⁸ The presence of glycosylated agrin, which is currently considered to be the major GBM HSPG, would have served to maintain normal physiologic ultrafiltration function in this model. However, the recent study reporting the production of a podocyte-specific agrin knockout mouse model, which led to the depletion of BM HS-GAGs associated with the agrin core protein, also showed little effect on overall glomerular morphology and renal function.¹⁹ Another approach used global expression of heparanase in a transgenic model²⁰ to enhance HS-GAG degradation. Analysis of the phenotype of the model showed intact HSPGs were still assembled and exported by cells, albeit processed by the active heparanase enzyme into a lower molecular weight species of PG. The net outcome in this transgenic model was only mild albuminuria.

The morphologic features seen in the PEXTKO mouse can be associated with several glomerular diseases, but appear to align with those described for minimal change glomerulopathy (MCG) in humans.²¹ MCG (also known as Minimal Change Nephrotic Syndrome) accounts for approximately 90% of nephrotic syndrome seen in juvenile patients under the age of 10 years and 50% of nephrotic syndrome in

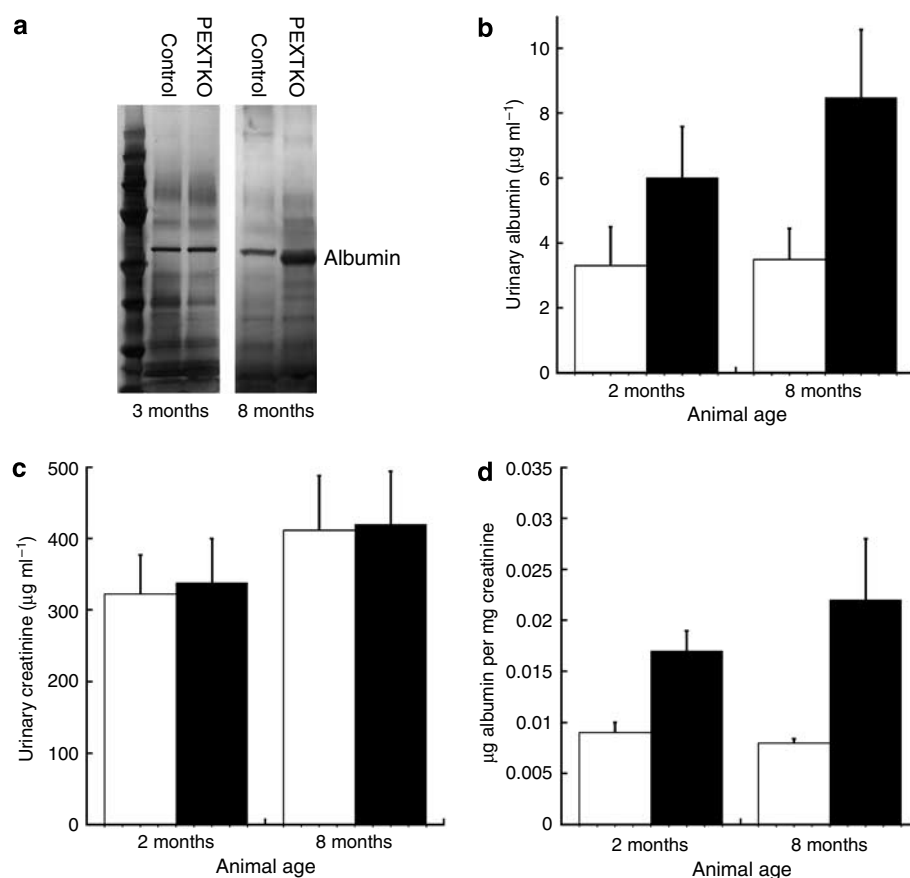


Figure 8 | (a) Silver-stained gel of urinary proteins from representative age-matched (3 months) control and PEXTKO animals (collection interval 24 h). At 3 months of age, there was no discernable difference in albumin between control and PEXTKO animals. At 8 months of age, a slight amount of albuminuria is present in the PEXTKO animals compared to control. In ELISA-based assays for urinary albumin, a slight increase in urinary albumin (b) was seen in PEXTKO animals at 2 and 8 months of age when compared to controls, albeit the differences did not reach statistical significance ($n = 5$ animals per group). Urinary creatinine levels (c), as measured by a commercially available plate assay, were comparable between both groups at both ages. The ratio of urinary albumin/creatinine (d) was increased in PEXTKO animals at both ages but the differences did not reach statistical significance.

juveniles beyond that age.²¹ The etiology of MCG in humans is not entirely clear and to some extent multifactorial (idiopathic or secondary) in nature.²¹ Although we are not proposing the PEXTKO mouse as a model for MCG since the mutant mouse does not mimic the etiology of MCG, it does exhibit several morphological changes that have been associated with MCG. Unlike MCG, however, severe proteinuria does not develop in PEXTKO mice. One key morphologic change seen in the PEXTKO mouse in common with MCG is the lack of obvious glomerular lesions in light microscopy but the presence of tubular epithelial cell changes. The observed glomerular ultrastructural changes are consistent with that reported for MCG and include podocyte foot process effacement, microvillous transformation but with relatively normal BM thickness.²¹ The basic lesion of the PEXTKO model, that is, the loss of the ability of the podocytes to synthesize and deliver intact HSPGs to the GBM also corresponds to some extent by previous studies in humans, which showed that in MCG there is a loss of GBM HS-GAGs without the loss of the agrin core protein.²²

In the case of the PEXTKO mouse, albuminuria detectable by SDS-polyacrylamide gel electrophoresis (PAGE) is coincident with loss of HS-GAG only after visible changes in the proximal tubules of the kidney are seen. However, ELISA-based assays showed that the PEXTKO mouse develops a slight but not statistically significant increase in urinary albumin excretion (Figure 8d) at 2 months of age that was not initially evident by SDS-PAGE. The same method of urinalysis of 8-month-old animals shows that the albuminuria is increased in PEXTKO mice compared to control animals (Figure 8d), an observation consistent with the SDS-PAGE data. However, the albuminuria seen at both 2 and 8 months was mild and did not reach statistical significance. In light of the discussion within one of the above paragraphs, which indicated that the loss of HS-GAG from the GBM may only have modest effects on overall ultrafiltration, led us to consider that the protein retrieval capacity of the proximal tubules in murine nephron might be greater than previously thought and proximal tubule elements could be capable of developing a compensatory response to handle a moderate degree of protein overload in younger PEXTKO animals. This

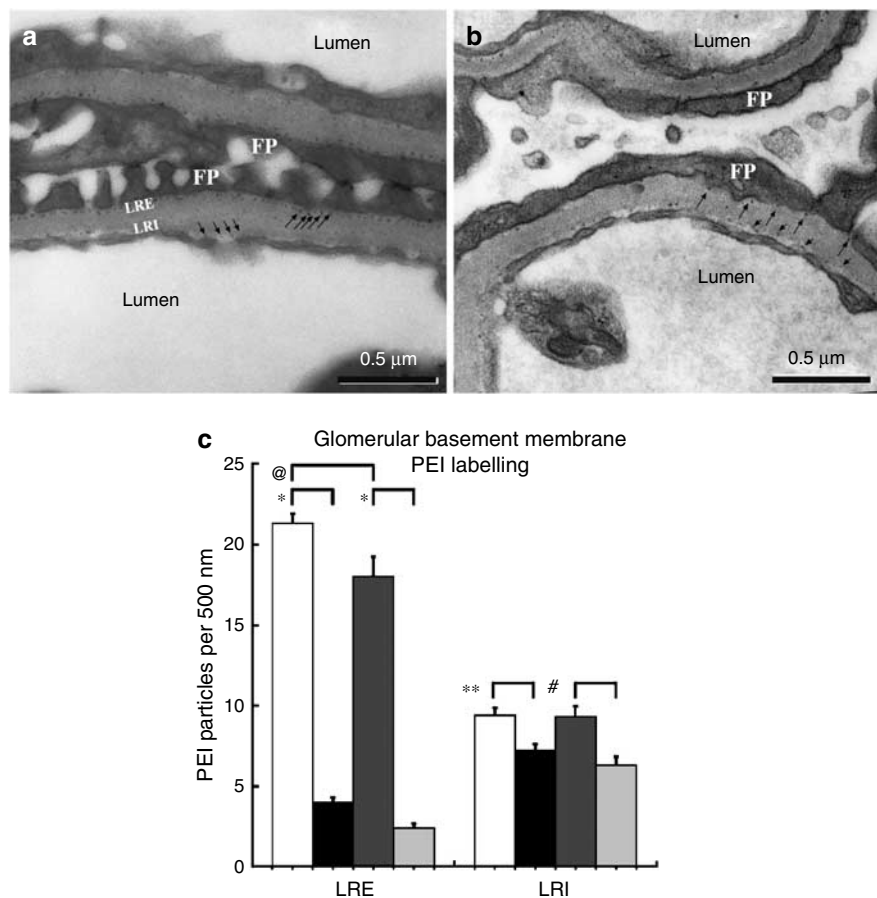


Figure 9 | The micrographs in (a, b) are of two adjacent glomerular capillary walls from control (a) and PEXTKO (b) animals (8 months of age shown) that were labeled with PEI, a probe for the presence of anionic sites in the GBM. In control animals, PEI label can be found immediately subtending the podocyte foot processes and endothelial cells (black arrows) in the lamina rara externa (LRE) and lamina rara interna (LRI), respectively. The labeling ratio for PEI in these areas is approximately 2:1 (LRE:LRI). The amount of PEI labeling in the PEXTKO animal is significantly decreased (black arrows). The graph in (c) compares the number of PEI sites in the LRE and LRI from control and PEXTKO kidneys of 2 and 8 months of age. The data show a significant decrease in the amount of PEI label in the LRE ($*P < 0.0001$) in both age groups. An age-related decrease in anionic sites in the LRE was also seen in control animals ($@P = 0.0004$). In the LRI of PEXTKO animals, a decrease in anionic sites was also seen at both 2 months ($**P = 0.0004$) and 8 months ($#P < 0.0019$) compared to controls. □ control 2 months, ■ PEXTKO 2 months, ▒ control 8 months, ◻ PEXTKO 8 months.

premise was recently buttressed in a study by Russo *et al.*²³ which used intravital multiphoton microscopy to show that albumin delivery to the normal rodent proximal tubule was greater than previously indicated by micropuncture studies. Their reported glomerular sieving coefficient of 0.034 suggests that levels of albumin that would be considered in the nephrotic range are actually routinely delivered to the proximal tubules on a daily basis. Thus, the proximal tubule epithelial cells are capable of retrieving a greater than anticipated protein load in normal animals, resulting in no measurable albuminuria. Further experiments in their report, which used a puromycin aminonucleoside nephrosis-induced nephritis rat model, showed that the development of proteinuria was coincident with a dysfunction in proximal tubule epithelial retrieval activity. Thus, it is possible in the PEXTKO model that some type of albumin retrieval mechanism becomes upregulated and compensates for an increased protein delivery to the tubule system. And, if this is

the case, then over time decompensation/defeat of this mechanism gradually occurs leading to the measurable albuminuria seen in our model.

The presence of podocyte foot process effacement despite no loss of HSPG core protein in PEXTKO mouse model strongly suggests that the HS-GAGs on HSPGs secreted by podocytes in some way have direct effects on the foot process organization of the glomerular podocytes. The fact that minor albuminuria develops several months prior to the observed tubule damage suggests that foot process effacement may be a contributing factor in our observations. The mechanism by which the HS-GAG loss affects podocyte foot process organization in the PEXTKO model is currently under investigation. Although one might speculate that a single molecular PG species could be the nidus of such changes, because of the diverse functions of PGs/GAGs the eventual answer could involve several different lines of reciprocal cell-matrix interactions. However, the fact that

the GBM-specific agrin knockout mouse does not develop foot process effacement,¹⁹ from the standpoint of cell–matrix interactions, would indicate that neither the presence of HS-GAGs on agrin nor the agrin core protein itself is critical in mediating foot process morphology. We believe that the podocyte phenotype in the PEXTKO animal might possibly be explained by a loss of ability of cell surface PGs, that is, members of the syndecan family,²⁴ to interact with HS-GAG binding proteins such as laminin, which are present in the GBM. In many cell systems, such as fibroblasts, syndecan–matrix interactions are important in the development of focal contacts/adhesions,²⁵ the primary syndecan involved in this system is syndecan-4, which has also been shown to be present in the glomerulus.²⁶ Although the biology of the syndecans has been well studied in other systems, little is known about syndecan biology in the podocyte. Preliminary data from our laboratory (S Chen and KJ McCarthy, unpublished results) show that the loss of EXT1 in immortalized podocytes results in loss of not only extracellular matrix associated HS-GAGs but also cell surface HS-GAGs. Thus, it is highly likely that in the PEXTKO mouse, the loss of cell surface HS-GAGS could be playing a role in directing podocyte behavior.

MATERIALS AND METHODS

Animals and animal care

Mice were housed under controlled conditions of light and humidity in the Animal Resource Facility, an Association for Assessment and Accreditation of Laboratory Animal Care-approved facility, at LSU Health Sciences Center. All experimentation in the studies was carried out under association for Assessment and Accreditation of Laboratory Animal Care-approved guidelines. Mice transgenic for a 2.5P-Cre expression (podocin-Cre⁺) construct were a gift from Dr Lawrence Holzman (University of Michigan, Ann Arbor, MI, USA).¹⁰ The Cre recombinase cassette in the expression construct was under control of the human podocin (NPHS2 gene) promoter permitting the expression of Cre recombinase specifically in glomerular podocytes. *Ext1*^{flox/flox} mice were a gift from Dr Yu Yamaguchi (Burnham Institute for Biomedical Research, La Jolla, CA, USA). The *Ext1* alleles in these mice are flanked by a *loxP* site inserted into 5' untranslated region of exon 1 (230 nucleotides upstream of the translation initiation site) and the other *loxP* site in the intron downstream of exon 1. Both sets of mice had been previously crossed with C57BL/6J mice to breed the mutations into the C57BL/6J genome background. Podocin-Cre⁺ mice were crossed with *Ext1*^{flox/flox} to get the Podocin-Cre/*Ext1*^{flox/-} mice, which were then backcrossed to get the Podocin-Cre/*Ext1*^{flox/flox} mice.

Murine genotyping

Genotyping was carried out by PCR of tail snips using REDExtract-N-Amp™ Tissue PCR Kit (Sigma Chemical, St Louis, MO, USA), using the primers 5'-GGAGTGTGGATGAGTTGAAG-3' (forward) and 5'-CAACACTTTCAGCTCCAGTC-3' (reverse).²⁷ Cycling parameters for PCR were 95°C, 15 min; 94°C 1 min, 55°C 1 min, 72°C 1 min, repeat 40 cycles: 72°C 10 min. Screening primers for podocin-Cre were 5'-GCATAACCAGTGAACAGCATTGCTG-3 (forward) and 5'-GGACATGTTTCAGGGATCGCCAGGCG-3 (reverse).²⁸ Cycling parameters for the PCR were 95°C, 15 min; 94°C 1 min, 54°C 1 min, 72°C 1 min, repeat 35 cycles: 72°C 10 min.

Immunohistochemistry

Unfixed renal tissue was embedded in OCT compound (Sakura Finetek USA Inc. Torrance, CA, USA), snap frozen and stored at -20°C until used and at -80°C for long-term storage. Sections (4 μm) were cut and affixed to glass slides. Immunohistochemistry was done as previously described.²⁹ For comparative purposes (see Microscopy and morphometric measures), age-matched kidney sections from control and PEXTKO animals were affixed to the same slide, permitting both sets of tissues to be immunostained under similar conditions, thus avoiding possible differences in staining intensity arising from variances in staining conditions. The following primary antibodies were used in the study: (1) anti-agrin (1:50, K-17:sc-6166; Santa Cruz Biotechnology, Santa Cruz, CA, USA) which recognizes an epitope present within the last 50 AA of agrin; (2) rat monoclonal anti-perlecan antibody (1:100, clone A7L6, Upstate Biotechnology, Lake Placid, NY, USA); (3) rat anti-laminin γ1 chain (Clone A5 1:100, Millipore Inc., Billerica, MA). (4) anti-HS (1:2, HS4C3). Antibody HS4C3 recognizes N- and O-sulfated HS domains, especially 3-O sulfated ones, which are typically present in the GBM.^{30–32} Primary antibodies were localized using species-specific Cy-2 or Cy-3-conjugated secondary antibody (1:100; Jackson Immuno-research Laboratories, West Grove, PA, USA). In the case of immunodetection on mouse tissues with phage display-derived antibodies (HS4C3), a monoclonal mouse anti-VSV antibody (1:100 clone P5D4; Sigma Chemical) conjugated to Cy-3 was used.

Glomerular C-6-sulfate GAG localization was done using a mouse monoclonal antibody, 3B3, which specifically recognizes a C-6-sulfate neo-epitope³³ present on C-6 PGs after prior treatment with chondroitinase ABC (0.4 U/ml; Seikagaku Corporation, Tokyo, Japan).

Microscopy and morphometric measures

Digital images of the specimens were acquired using an Olympus IX-70 microscope equipped for epifluorescent illumination. The microscope was interfaced to a Hamamatsu Orca camera (Hamamatsu, Bridgewater, NJ, USA), the signal from which was ported to a Macintosh Power PC hosting the imaging acquisition/analysis software I-Vision-Mac (BioVision Technologies, Exton, PA, USA). To determine differences in relative fluorescence intensity between age-matched control and PEXTKO animals, slides with age-matched control and PEXTKO paired tissue sections were immunostained as described above to ensure consistency of immunoreagents during the staining process. During imaging, the length of camera exposure was set to the brightest immunofluorescence intensity between the two specimens to limit pixel saturation. Subsequent imaging of both paired specimens was done at the set exposure. Morphometric measures of glomerular area on frozen sections (20 glomeruli per animal, three animals per group) were done using a planimetry subroutine in I-Vision-Mac as previously described.³⁴ Microtome digital deconvolution software (Vaytek Inc., Fairfield, IA, USA) was used to deconvolve 0.1 μm-step image stacks of serially acquired focal planes to generate confocal images of immunostained glomeruli (Figure 4a–f).

In vivo labeling of anionic sites

To further investigate changes in the density of polyanionic sites in the GBM of glomeruli from PEXTKO animals compared to control animals, three animals per group (2 and 8 months of age) were injected intracardially with 50 μl of a 0.5% polyethyleneimine solution (average molecular weight 25 000; Polysciences, Warrington, PA, USA) in a manner similar to that described by Schurer *et al.*³⁵ At 1 h post-injection, the animals were killed, the kidneys were removed and processed for electron microscopy studies (see below).

Electron microscopy

Electron microscopy studies were done as previously described.³⁶ Briefly, kidneys from control and PEXTKO mice were minced in 1 mm² pieces and fixed in 2.5% glutaraldehyde and 2% formaldehyde in 0.1 M Sorenson's phosphate buffer (pH 7.4) overnight followed by postfixation in 2% osmium tetroxide in 0.1 M Sorenson's phosphate buffer for 2 h. Subsequently, the tissues were dehydrated in a graded series of ethanol and propylene oxide solutions and embedded in epoxy resin (Durcupan ANC Fluka Araldite; Sigma Chemical). Tissue sections were cut at 80 nm thickness using a Reichert Ultracut E Ultramicrotome (Leica Microsystems, Bannockburn, IL, USA) and stained with uranyl acetate and lead citrate as previously described.³⁶ Specimens were imaged using a Phillips CM-10 electron microscope. For quantification of BM labeling, a grid corresponding to 500 nm × 500 nm squares was superimposed over scanned electron micrographs. The number of PEI particles per 500 nm length of GBM were counted for three capillary walls per glomerulus from five glomeruli from each animal.

Urinalysis

For SDS-PAGE analysis of urinary proteins, urine was either collected at the time of killing (acute) or for 24 h urinary excretion, mice were housed in metabolic cages (Nalgene, Nalge Nunc International, Rochester, NY, USA). For SDS-PAGE analysis, 20 µl of urine from transgenic or control mice was electrophoresed on a 4–12% SDS-PAGE gel (Invitrogen, Carlsbad, CA, USA) followed by silver staining. Images of the gels were digitized using a Kodak 2000MM imaging workstation. For additional urinalysis, spot urines were collected from control and PEXTKO mice (2 and 8 months of age, five animals per group). Urinary albumin was measured by ELISA according to the manufacturer's instructions (Albuwell M; Exocell, Philadelphia, PA, USA); urinary creatinine was done using a modified alkaline picrate method (Creatinine Companion; Exocell) according to the manufacturer's instructions.

Statistical analysis

Statistical analysis was done by ANOVA with *post hoc* testing (Bonferroni–Dunn test) using the Statview software package.

DISCLOSURE

All the authors declared no competing interests.

ACKNOWLEDGMENTS

This study was supported in part by grants from NIH/NIDDK (1-RO1-DK48055, KJM) and the Netherlands Organization for Scientific Research (NWO Program Grant 902-27-292, TvK) and the International Human Frontier Science Program Organization (HFSP, Grant RGPO062/2004-C101, TvK). We thank Mr Ronald Austin, Department of Pathology LSUHSC-S, for his assistance with the CM-10 electron microscope, Dr Gregory Lautenslager (Exocell) for his helpful discussions concerning the urinalysis, Ms Beth Hickman for her management of our mouse colony, and Dr Stephen Bonsib, Chairman, Department of Pathology LSUHSC-S, for departmental support.

Note: A recent report by Roberts and Gleadle (JASN doi: 10.1681/ASN.2007080842, published online 23 January 2008) demonstrated a renal phenotype in the case of a 37-year-old woman with hereditary multiple exostoses (HMEs). Sequencing of the EXT1 gene from this patient showed a type 2 frameshift mutation (238 delA), which would affect the downstream gene product from the affected allele. The patient presented with peripheral edema had 24 g/dl proteinuria, 23 g/l albuminuria, and a serum creatinine of 1.1 mg/dl. Renal biopsy showed mesangial expansion, accumulation of fibrillar collagen in the mesangium and capillary walls, and modest podocyte foot process

effacement. In comparison to the mouse data in our report, both phenotypic and functional changes reported in the case study are far more severe. This difference could be a reflection of the fact that in the human condition of HME, there would be a global haploinsufficiency of the expression of EXT1 within all cells that would normally express EXT1 in the patient. More likely than not, HS-GAG assembly in mesangial cells would also be affected in HME. In our model, *Ext1* is not affected in mesangial cells since they remain capable of assembling HS-GAG (Figure 4). Although the glomeruli from the PEXTKO mouse undergo hypertrophy, mesangial expansion does not occur in the PEXTKO glomeruli (S Chen and KJ McCarthy, unpublished results). Thus, the loss of EXT1 activity in mesangial cells may be directly contributory to the progression of mesangial expansion seen in the case study.

SUPPLEMENTARY MATERIAL

Figure S1.

Supplementary material is linked to the online version of the paper at <http://www.nature.com/ki>

REFERENCES

1. Iozzo RV, Murdoch AD. Proteoglycans of the extracellular environment: clues from the gene and protein side offer novel perspectives in molecular diversity and function. *FASEB J* 1996; **10**: 598–614.
2. Esko JD, Selleck SB. Order out of chaos: assembly of ligand binding sites in heparan sulfate. *Annu Rev Biochem* 2002; **71**: 435–471.
3. Cattaruzza S, Perris R. Proteoglycan control of cell movement during wound healing and cancer spreading. *Matrix Biol* 2005; **24**: 400–417.
4. Kanwar YS, Linker A, Farquhar MG. Increased permeability of the glomerular basement membrane to ferritin after removal of glycosaminoglycans (heparan sulfate) by enzyme digestion. *J Cell Biol* 1980; **86**: 688–693.
5. Kim BT, Kitagawa H, Tamura J *et al.* Human tumor suppressor EXT gene family members EXTL1 and EXTL3 encode alpha 1,4-N-acetylglucosaminyltransferases that likely are involved in heparan sulfate/heparin biosynthesis. *Proc Natl Acad Sci USA* 2001; **98**: 7176–7181.
6. Busse M, Kusche-Gullberg M. *In vitro* polymerization of heparan sulfate backbone by the EXT proteins. *J Biol Chem* 2003; **278**: 41333–41337.
7. Abrahamson DR. Structure and development of the glomerular capillary wall and basement membrane. *Am J Physiol* 1987; **253**: 783–794.
8. St John PL, Abrahamson DR. Glomerular endothelial cells and podocytes jointly synthesize laminin-1 and -11 chains. *Kidney Int* 2001; **60**: 1037–1046.
9. Inatani M, Irie F, Plump AS *et al.* Mammalian brain morphogenesis and midline axon guidance require heparan sulfate. *Science* 2003; **302**: 1044–1046.
10. Moeller M, Sanden S, Soofi A *et al.* Podocyte-specific expression of Cre recombinase in transgenic mice. *Genesis* 2003; **35**: 39–42.
11. Noakes PG, Miner JH, Gautam M *et al.* The renal glomerulus of mice lacking laminin/lamin B2: nephrosis despite molecular compensation by laminin B1. *Nat Genet* 1995; **10**: 400–406.
12. van Kuppevelt TH, Dennissen MA, van Venrooij WJ *et al.* Generation and application of type-specific anti-heparan sulfate antibodies using phage display technology. Further evidence for heparan sulfate heterogeneity in the kidney. *J Biol Chem* 1998; **273**: 12960–12966.
13. Abrahamson DR, Perry EW. Evidence for splicing new basement membrane into old during glomerular development in newborn rat kidneys. *J Cell Biol* 1986; **103**: 2489–2498.
14. Wijnhoven TJ, Lensen JF, Wismans RG *et al.* *In vivo* degradation of heparan sulfate in the glomerular basement membrane does not result in proteinuria. *J Am Soc Nephrol* 2007; **18**: 3119–3127.
15. Seiler MW, Rennke HG, Venkatachalam MA *et al.* Pathogenesis of polycation-induced alterations ('fusion') of glomerular epithelium. *Lab Invest* 1977; **36**: 48–61.
16. Kelley VE, Cavallo T. Glomerular permeability: transfer of native ferritin in glomeruli with decreased anionic sites. *Lab Invest* 1978; **39**: 547–553.
17. Rossi M, Morita H, Sormunen R *et al.* Heparan sulfate chains of perlecan are indispensable in the lens capsule but not in the kidney. *EMBO J* 2003; **22**: 236–245.
18. Morita H, Yoshimura A, Inui K *et al.* Heparan sulfate of perlecan is involved in glomerular filtration. *J Am Soc Nephrol* 2005; **16**: 1703–1710.
19. Harvey SV, Jarad G, Cunningham J *et al.* Disruption of glomerular basement membrane charge through podocyte-specific mutation of agrin does not alter glomerular permselectivity. *Am J Pathol* 2007; **171**: 139–152.

20. Zcharia E, Metzger S, Chajek-Shaul T *et al.* Transgenic expression of mammalian heparanase uncovers physiological functions of heparan sulfate in tissue morphogenesis, vascularization, and feeding behavior. *FASEB J* 2004; **18**: 252–263.
21. Falk RJ, Jennette JC, Nachman PH. Primary glomerular disease. In: Brenner BM (ed). *Brenner & Rector's; The Kidney*, vol. 2, 6th edn. W.B. Saunders: Philadelphia, 2000, pp 1263–1349.
22. van den Born J, van den Heuvel LP, Bakker MA *et al.* Distribution of GBM heparan sulfate proteoglycan core protein and side chains in human glomerular diseases. *Kidney Int* 1993; **43**: 454–463.
23. Russo LM, Sandoval RM, McKee M *et al.* The normal kidney filters nephrotic levels of albumin retrieved by proximal tubule cells: retrieval is disrupted in nephrotic states. *Kidney Int* 2007; **71**: 504–513.
24. Woods A. Syndecans: transmembrane modulators of adhesion and matrix assembly. *J Clin Invest* 2001; **107**: 935–941.
25. Couchman JR, Woods A. Syndecans, signaling, and cell adhesion. *J Cell Biochem* 1996; **61**: 578–584.
26. Yung S, Woods A, Chan TM *et al.* Syndecan-4 up-regulation in proliferative renal disease is related to microfilament organization. *FASEB J* 2001; **15**: 1631–1633.
27. Inatani M, Irie F, Plump AS *et al.* Mammalian brain morphogenesis and midline axon guidance require heparan sulfate. *Science* 2003; **302**: 1044–1046.
28. Cushman LJ, Burrows HL, Seasholtz AF *et al.* Cre-mediated recombination in the pituitary gland. *Genesis* 2000; **28**: 167–174.
29. McCarthy KJ, Couchman JR. Basement membrane chondroitin sulfate proteoglycans: localization in adult rat tissues. *J Histochem Cytochem* 1990; **38**: 1479–1486.
30. Edge AS, Spiro RG. Characterization of novel sequences containing 3-O-sulfated glucosamine in glomerular basement membrane heparan sulfate and localization of sulfated disaccharides to a peripheral domain. *J Biol Chem* 1990; **265**: 15874–15881.
31. Ten Dam GB, Kurup S, van de Westerlo EM *et al.* 3-O-Sulfated oligosaccharide structures are recognized by anti-heparan sulfate antibody HS4C3. *J Biol Chem* 2006; **281**: 4654–4662.
32. Wijnhoven TJ, Lensen JF, Rops AL *et al.* Aberrant heparan sulfate profile in the human diabetic kidney offers new clues for therapeutic glycomimetics. *Am J Kidney Dis* 2006; **48**: 250–261.
33. Caterson B, Christner JE, Baker JR *et al.* Production and characterization of monoclonal antibodies directed against connective tissue proteoglycans. *Fed Proc* 1985; **44**: 386–393.
34. McCarthy KJ, Routh RE, Shaw W *et al.* Troglitazone halts diabetic glomerulosclerosis by blockade of mesangial expansion. *Kidney Int* 2000; **58**: 2341–2350.
35. Schurer JW, Hoedemaeker J, Molenaar I. Polyethyleneimine as tracer particle for (immuno) electron microscopy. *J Histochem Cytochem* 1977; **25**: 384–387.
36. McCarthy KJ, Bynum K, St John PL *et al.* Basement membrane specific chondroitin sulfate proteoglycan is abnormally associated with the glomerular capillary basement membrane in diabetic rats. *J Histochem Cytochem* 1994; **42**: 473–484.